

Multiphysics Approach to Numerical Modeling of a Permanent-Magnet Tubular Linear Motor

Ioana-Cornelia Vese, Fabrizio Marignetti, *Senior Member, IEEE*, and Mircea M. Radulescu, *Senior Member, IEEE*

Abstract—This paper presents a multiphysics modeling through finite-element (FE) coupled electromagnetic and thermal field analysis of a permanent-magnet tubular linear motor (PMTLM). Two-dimensional axial-symmetric FE steady-state and transient solutions are first obtained for the magnetic-flux-density distribution, cogging force, thrust, and losses of the PMTLM prototype. The FE magnetic field results are then used for the 3-D FE thermal simulation to get the PMTLM temperature distribution. This paper proves that the multiphysics numerical field analysis is a viable tool for the design and performance optimization of PMTLMs. The accuracy of the proposed study has been assessed through prior analytical and experimental results. Regarding the design aspects, some peculiarities in the thermal behavior of PMTLMs are emphasized. Generally, thermal models being not ready to develop, experimental and analytical solutions remain a preferred choice.

Index Terms—Coupled magnetic and thermal field analysis, finite-element (FE) modeling, permanent-magnet (PM) motor, tubular motor.

I. INTRODUCTION

AN INCREASED number of applications entail the simultaneous solving of two or more related physical phenomena. These applications require fast interdependent solutions, where there has been no previous knowledge, and the multiphysics solver could make up the early stage of a design optimization process. In this paper, the electromagnetic features of a permanent-magnet (PM) tubular linear motor (PMTLM) team up with the thermal ones in order to achieve the coupled-field analysis of the motor.

Linear electromagnetic motors are being used in applications ranging from manufacturing automation and transportation to healthcare and household appliances.

Providing thrust force directly to a payload, they offer numerous advantages over rotary-to-linear counterparts, notably the absence of mechanical gears and transmission systems, which results in higher efficiency, better dynamic performance, and improved reliability.

Among various linear motor topologies [1], PMTLMs emphasize high power density, high thrust capability, and excellent

TABLE I
MAIN DESIGN AND OPERATIONAL PARAMETERS
OF THE PMTLM PROTOTYPE

Pole pitch	60 [mm]
Slot pitch	20 [mm]
Number of phases	3
Number of pole pairs	4
Maximum speed	2.2 [m/s]
Stator length	0.30 [m]
Stator outer radius	0.064 [m]
Stator inner radius	0.03 [m]
Stroke length	0.15 [m]
Rated voltage	40 [V]
Rated current	2 [A]

servo characteristics, having no end windings and zero net attractive force between stator and translator.

Any industrial applications require an appropriate thermal model, since it determines the admissible current density for its operational mode and the heat transfer imposes the restrictions for the motor power. Generally, it represents a complex problem that groups the identification of the encountered thermal phenomena, the definition of the heating sources, and the development of a suitable thermal model [2]–[5].

In order to obtain an optimized design and higher dynamic performances of the PMTLM, a coupled magnetic and thermal field analysis through a finite-element (FE) software-based multiphysics modeling is required. Hence, the aim of this paper is a multiphysics approach to PMTLM with an insight into the interaction between its magnetic and thermal behaviors. In [5]–[9], the authors offer models of coupling electromagnetic and thermal features by means of multiphysics design methodology for other motor topologies.

For the estimation of temperature distribution in different parts of a PMTL generator and the optimization of its performances, in [5], a combined electromagnetic–thermal model is developed, whereas in [10], the time effectiveness of the procedure is improved by using the space-mapping-based technique.

In the PMTLM coupled-field analysis adopted in this paper, the outcomes of the magnetic field analysis are applied as sources for the subsequent thermal analysis. Final results are validated against some analytical and experimental solutions for the most important quantities, such as iron losses, Joule losses, contact thermal resistances, and temperature distribution.

The study is based on a prototype PMTLM, built in the Laboratory of Industrial Electronics, University of Cassino, Cassino, Italy, whose main design and operational parameters are given in Table I.

Manuscript received February 28, 2009; revised August 3, 2009. First published September 1, 2009; current version published December 11, 2009.

I.-C. Vese and M. M. Radulescu are with the Special Electric Machines and Light Electric Traction Group, Technical University of Cluj-Napoca, 400020 Cluj-Napoca, Romania (e-mail: ioana.vese@edr.utcluj.ro; mircea.radulescu@mae.utcluj.ro).

F. Marignetti is with the Dipartimenti Automazione, Elettromagnetismo, Ingegneria dell'Informazione e Matematica Industriale, University of Cassino, 03043 Cassino, Italy (e-mail: marignetti@unicas.it).

Color versions of one or more of the figures in this paper are available online at <http://ieeexplore.ieee.org>.

Digital Object Identifier 10.1109/TIE.2009.2030206

It is a three-phase PMTLM, consisting of a laminated ferro-magnetic stator with ring-shaped copper coils inserted into the slots and a translator having successive iron and axially magnetized NdFeB PM rings.

II. MAGNETIC FIELD FE MODELING

Simulations by means of FE analysis represent a crucial stage of the motor optimal design, in order to determine the physical effects responsible for the PMTLM's behavior. The geometry to be modeled represents a small part of the entire model of the motor, and the connection between FEs creating the discretized field model is made automatically.

Using the JMAG-Studio software, 2-D nonlinear magnetic field FE simulations were performed by taking into account the axial symmetry of the PMTLM structure. During the numerical simulations, the steady-state and transient operations of the motor were fully considered.

The imposed physical properties of the materials and corresponding conditions for the field analysis ensure the accurate evaluation of global electromagnetic quantities, such as leakage and fringe fluxes. Some analytical procedures were integrated into the FE computations in order to yield general design guidelines.

The magnetic field distribution is analyzed under no-load and rated-load operating conditions, by transient time-stepped simulations, correlated with the imposed velocity on the translator and the current waveform through the coils. The JMAG-Studio iron loss tool enables the calculation of the iron loss distribution and loss amount based on the postprocessing of the magnetic field solution. The iron loss calculation uses analytically determined coefficients, i.e.,

$$W_{\text{loss}} = nB^{1.6}f^{1.6} + kB^2f^2 \quad (1)$$

where W_{loss} is the loss volume density (in W/m^3), B is the magnetic flux density (in tesla), f is the frequency (in hertz), n is the Steinmetz hysteresis loss coefficient (in J/m^3), and k is the eddy-current loss coefficient.

The FE simulations of the PMTLM magnetic behavior were carried out first under no-load operating conditions and then under rated-load conditions by imposing active magnets and sinusoidal current sources.

The FE simulation model of the PMTLM under rated-load operating conditions is shown in Fig. 1.

The distribution of the obtained magnetic flux density is shown in Fig. 2.

Then, the measurement of L_q and L_d is done, emphasizing the steps that were made. First, the translator was appropriately mounted, the magnets were replaced by air, and the values of current densities in various slots were set so that the generated magnetic flux is aligned to the d -axis.

The flux was calculated, thus allowing the determination of inductances on d and q axes. Results are listed in Table II.

From the performed simulations, one can notice that the iron parts are not saturated, due to the low magnetic flux density in the air gap. During the last simulation, thrust is FE computed, as shown in Fig. 3.

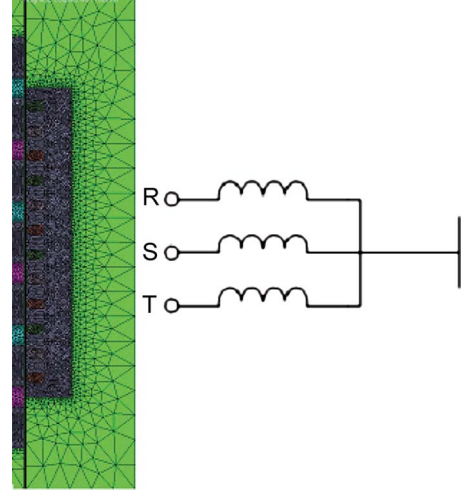


Fig. 1. Load 2-D axial-symmetric model of the PMTLM.

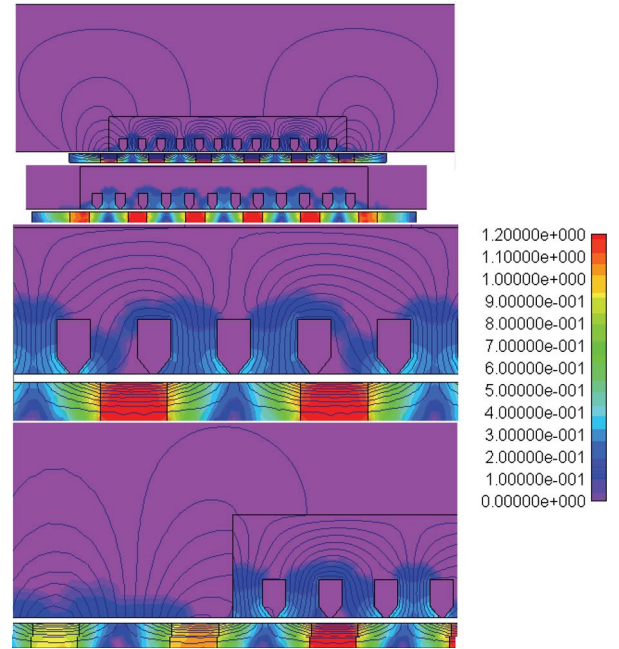


Fig. 2. FE-computed magnetic-flux-density distribution in the PMTLM under no-load conditions, for different positions of the translator.

TABLE II
VALUES OF THE INDUCTANCES

Current [A]	J [A/m ²]	Ld [mH]	Lq [mH]
1	763923.115	23.5	73.8
2	1527846.229	23.5	73.8
3	2291769.345	23.5	73.8
4	3055692.459	23.5	73.8
5	3819615.574	23.5	73.8

Under analytical approach, iron losses, although difficult to approximate, are calculated as in (1) with the magnetic hysteresis and classical eddy currents taken into account, whereas the excess eddy-current component is neglected.

The instantaneous copper loss may be expressed as

$$P_{\text{Cu}} = 3 \cdot R_0 \cdot i^2 \cdot [1 + \alpha(T - T_a)] \quad (2)$$

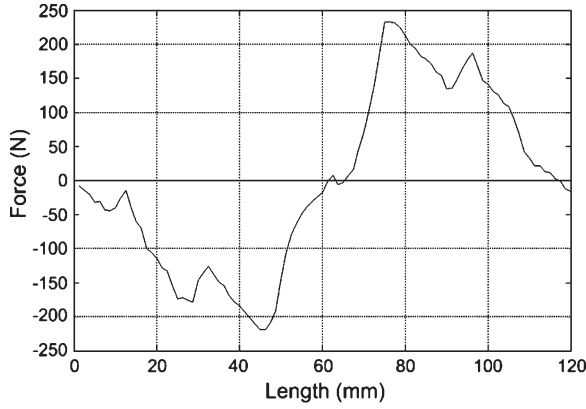


Fig. 3. FE-computed thrust of the PMTLM prototype.

where i is the current, T_a is the ambient temperature, R_0 is the phase resistance measured at the base temperature, T is the actual temperature, and α is the temperature coefficient.

Out of the carried simulations, the resulted global loss quantity will be considered as the main source of thermal energy into the corresponding FE thermal model.

III. THERMAL MODELING

The energy dissipation in the PMTLM is due to hysteresis and eddy-current iron losses, as well as to Joule losses in the windings. It causes the heating of various parts of the motor, affecting the electric life and the dielectric properties of insulation.

Already carried-out analytical studies on the PMTLM thermal model [6] highlighted the contributions of Joule and iron losses to the temperature distribution.

A. Thermal Equivalent-Circuit Model

Two thermal phenomena are taken into account when studying the thermal behavior of PMTLM prototype: natural convection and conduction.

The natural convection is considered between the external surface of the PMTLM and the environment, caused mainly by the density difference coming from the temperature gradient. The calculation of the mean convection heat transfer coefficient is based on empirical nondimensional numbers depending on the convection type, i.e., Prandtl P_r and Rayleigh R_a numbers for the free convection. These numbers define the Nusselt number N_u , which gives the mean convection heat transfer coefficient h_c

$$h = \frac{N_u \cdot k}{l} \quad (3)$$

where k is the thermal conductivity of the air, and L represents the length of the PMTLM in contact with the air. The corresponding thermal resistance R_h is described by

$$R_h = \frac{l}{h \cdot A} \quad (4)$$

where l is the specific length of the motor (in meters), h defines the natural convection coefficient (in $\text{W}/\text{m}^2 \cdot ^\circ\text{C}$), and A represents the area in contact to the environment (in m^2).

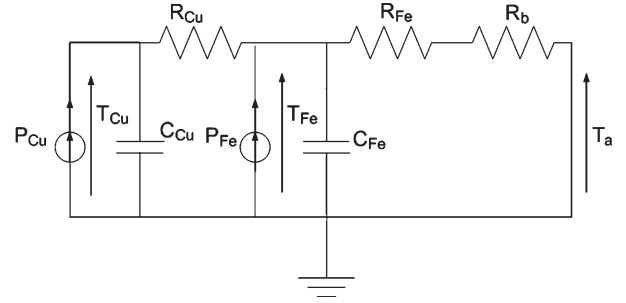


Fig. 4. Thermal equivalent circuit of the PMTLM under transient operation.

Thermal conduction represents a transport of energy in a medium, due to a temperature gradient. The thermal resistances of copper and iron are conduction resistances given by

$$R_{\text{Cu,Fe}} = \frac{L_{\text{Cu,Fe}}}{\lambda_{\text{Cu,Fe}} \cdot A_{\text{Cu,Fe}}} \quad (5)$$

where $L_{\text{Cu,Fe}}$ (m) and $A_{\text{Cu,Fe}}$ (m^2) are the specific length and area of the copper and iron, respectively, and $\lambda_{\text{Cu,Fe}}$ ($\text{W}/\text{m} \cdot ^\circ\text{C}$) represents the thermal conductivity of the material.

The thermal capacitances are modeled by the next quantities

$$C = \rho \cdot V \cdot c \quad (6)$$

where ρ defines the mass density of the considered object (in kg/m^3), V is its volume (in m^3), and c is its specific heat (in $\text{kJ}/\text{kg} \cdot ^\circ\text{C}$). At steady-state conditions, all capacitors are deleted from the thermal model.

A complex thermal model of a PMT machine must take into account all the exothermal parts, resulting into a complicated network of thermal resistances and capacitors. For the sake of simplicity, a 1-D model is adopted for the analytical study. In this case, one deals with two main loss sources: copper loss P_{Cu} and iron loss P_{Fe} .

These losses yield the thermal resistances of the winding, iron, and environment. The whole model is shown in Fig. 4 with reference to the transient state of the PMTLM machine. Capacitors are included in the thermal network, accounting for the thermal capacitances of the materials.

In the thermal model, T_{Cu} denotes the temperature of the windings; T_{Fe} is the temperature of the iron; T_h is the temperature of the environment, assumed equal to 23°C ; and C_{Cu} and C_{Fe} define the thermal capacitances of copper and iron, respectively.

The differential equations associated to the thermal model are iteratively solved, and they yield the temperatures in PMTLM, in the dependence of copper and iron losses calculated at each time step, until thermal steady-state behavior is reached. Temperature values change slowly in time due to the thermal capacitance effect. The analytically obtained values of resistances and capacitances, in the thermal network of Fig. 4, are given in Table III.

The thermal resistance of the windings was obtained, considering the air spaces between wires and the insulation. The wires were insulated with enamel paint, impregnated with epoxy and externally insulated with Kapton tape.

TABLE III
VALUES OF RESISTANCES AND CAPACITANCES
OF THE THERMAL NETWORK

Parameter	Value
R_h	0.6942 [K/W]
R_{Cu}	0.1189 [K/W]
R_{Fe}	0.0218 [K/W]
C_{Cu}	369 [J/K]
C_{Fe}	7207.6 [J/K]

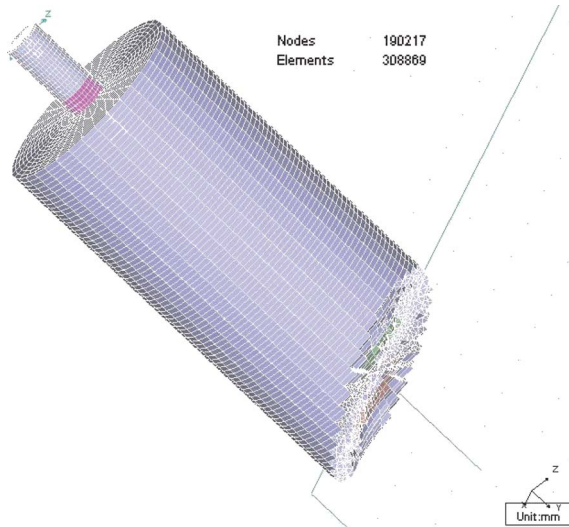


Fig. 5. Three-dimensional thermal model of the PMTLM.

B. Thermal Field FE Modeling

When analyzing by means of FE, a 3-D thermal model is created [11], accounting for all the releasing heat parts of the motor, with the corresponding heat losses and transfer coefficients.

The heat transfer in a material should take into account the physical properties of the used material: thermal conductivity, specific heat, and mass density. Table III shows some of these parameters. Although thermal Field FE modeling requires a 3-D FE model, this yields a large number of nodes and iterations. Therefore, only a part of the entire model will be implied in the final simulation.

Fig. 5 shows the 3-D thermal model of the PMLTM, as designed using the JMAG-Studio software.

In order to obtain a thermal field solution, the transfer boundary regions and heat sources must be defined in the 3-D model, as explained in the next chapter.

The peculiarity of the PMTLM seems to be the involvement of the slider in the heat exchange with the ambient, during its alternative linear motion.

IV. MULTIPHYSICS FE MODELING AND SIMULATIONS

Coupled-field analysis takes into account two or more physical phenomena; they can be considered simultaneously or by putting one's postprocessed information into the other's solution. Accordingly, the multiphysics tools can handle two ways of field coupling, depending on the directions of solving.

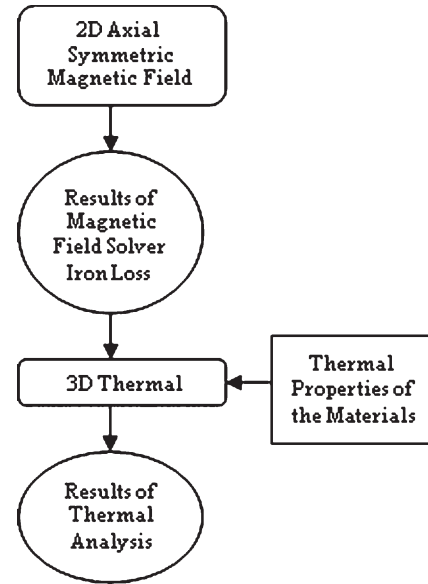


Fig. 6. Sequential magnetothermal coupling.

TABLE IV
THERMAL PROPERTIES OF THE USED MATERIALS DURING SIMULATIONS

Material	Thermal conductivity [w/m ⁰ K]	Specific heat [J/kg ⁰ K]	Density [kg/m ³]
Iron	80.2	440	7874
Copper Coils	401	385	8960

The one-direction coupling is a sequential method that consists in separately running two types of analyses for different fields and applying the results obtained in one analysis as an input for the other one [12].

The direct method or the coupling in both directions refers to the case in which analyses are executed simultaneously by conducting the handle of information mutually.

After running the magnetic analysis, the iron loss result is loaded into the 3-D thermal model as the main heat generation source (Fig. 6), and the analysis is conducted in a transient time-stepped mode. The corresponding thermal resistances are also set into the FE model, and the natural convection is set as a boundary transfer condition with a proper coefficient. The material behavior with respect to temperature, the thermal conductivity, specific heat, and the density of materials are suitably chosen into the model, as shown in Table IV. In order to obtain the thermal solution, boundary conditions and heat sources must be defined.

The average temperatures obtained by FE simulation for different parts of the PMLTM are shown in Fig. 7, and in Fig. 8, the plot of temperature distribution in the PMTLM is shown.

As expected, the temperatures in the copper regions are higher than in iron parts, because of the larger Joule loss generated in the stator winding.

The thermal analysis of PMTLM and temperature distribution in several motor parts is validated against the experimental results obtained prior to the multiphysics approach.

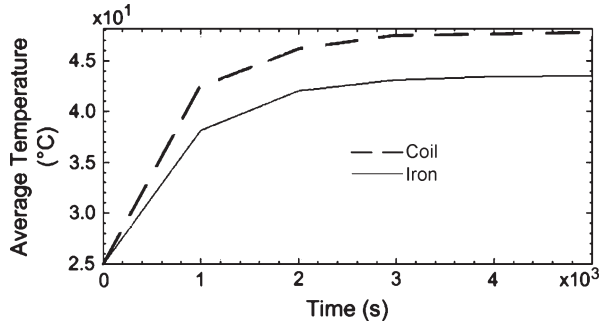


Fig. 7. Average simulated temperatures in one coil winding and stator iron.

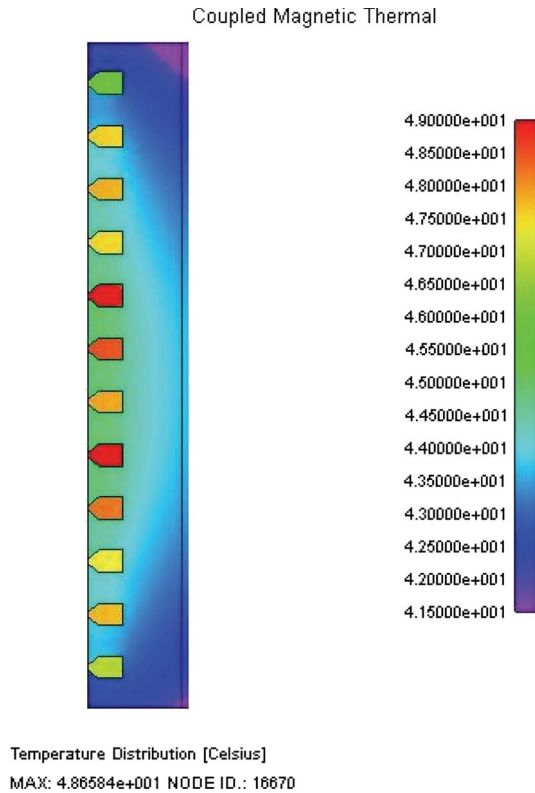


Fig. 8. Simulated temperature distribution in the stator iron and windings.

V. EXPERIMENTAL RESULTS

The PMTLM prototype, having the main parameters and design data given in Table I, was used to experimentally check its thermal behavior. All experiments have been performed in the Laboratory of Industrial Electronics, University of Cassino.

Two thermocouples have been mounted on the PMTLM prototype, one at the outer surface of the stator and the other one is embedded in the windings. As the temperatures change slowly, the measurements were recorded for 2 h.

The tests were done with the machine operating in generator mode. A test rig was built using a brushless motor drive to produce alternative motion.

In the beginning, the heat exchange was considered strictly in the stator, through the external surface of the iron cylinder. This was taken into account by

$$A_{Fe} = 2 \cdot \pi \cdot r_{Fe} \cdot L_{Fe} \quad (7)$$

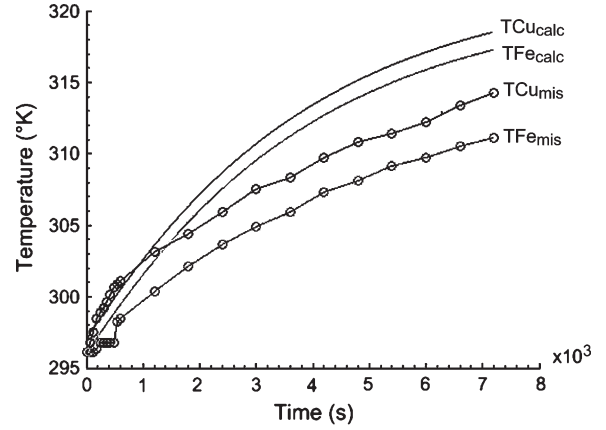


Fig. 9. Calculated and measured temperatures.

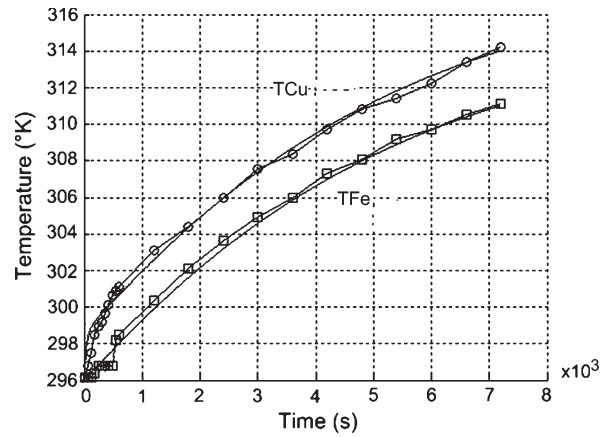


Fig. 10. Calculated and measured temperatures of copper and iron parts.

where r_{Fe} represents the stator outer radius, and L_{Fe} denotes the stator axial length.

The simulations obtained under these assumptions were compared with the experimental results, as shown in Fig. 9.

As noticed, if one considers just the outer surface of the stator, the simulated and measured temperatures will not fit well. Hence, the concerned iron surface of the outer stator has to be enlarged, as

$$A_{Fe} = 2 \cdot \pi \cdot r_{Fe} \cdot L_{Fe} + 2 \cdot \pi \cdot r_{in} \cdot L_{stroke} \quad (8)$$

The effect of the inner tube, moving alternatively, is to conduct outside the heat it receives via the air gap and, finally, to dissipate it within the ambient environment.

Fig. 10 shows the sample temperatures measured through thermocouples and the ones obtained from the improved mathematical model; it can be seen that they are now in good agreement, which confirms the analytical solution obtained for the PMTLM regions involved in the heat exchange.

VI. CONCLUSION

A multiphysics approach to FE field analysis of PMTLM represents a crucial stage of motor design optimization and performance improvement for industrial applications.

The studies of electromagnetic and thermal behaviors have been done for PMTLM prototype, using analytical-experimental and multiphysics approaches. The obtained results contribute to a good characterization of PMTLM magnetothermal behavior, revealing valuable information for the design optimization process.

The FE simulations of the coupled magnetothermal behavior of PMTLM represent a valuable tool in properly combining the effects of both physical phenomena, hence offering a global display of PMTLM performances.

REFERENCES

- [1] F. Marignetti and M. Scarano, "Comparative analysis and design criteria of permanent magnet tubular actuators," *Elect. Eng.*, vol. 84, no. 5, pp. 255–263, Dec. 2002.
- [2] P. H. Mellor, D. Roberts, and D. R. Turner, "Lumped parameter thermal model for electrical machines of TEFC design," *Proc. Inst. Elect. Eng.—Elect. Power Appl.*, vol. 138, no. 5, pp. 205–218, Sep. 1991.
- [3] B. Alvarenga, "Thermal characterization of long electrical devices—Application to a tubular linear induction motor," in *Proc. IEMDC*, Jun. 2003, vol. 2, pp. 938–942.
- [4] D. Staton, A. Boglietti, and A. Cavagnino, "Solving the more difficult aspects of electric motor thermal analysis in small and medium size industrial induction motors," *IEEE Trans. Energy Convers.*, vol. 20, no. 3, pp. 620–628, Sep. 2005.
- [5] S. R. Adi, W. N. L. Mahadi, and K. M. Nor, "Thermal analysis of a tubular permanent magnet linear generator using multiphysics solver," in *Proc. IEEE Region 10 TENCON Conf.*, Nov. 2005, pp. 1–6.
- [6] L. Alberti and N. Bianchi, "A coupled thermal-electromagnetic analysis for a rapid and accurate prediction of IM performance," *IEEE Trans. Ind. Electron.*, vol. 55, no. 10, pp. 3575–3582, Oct. 2008.
- [7] F. Marignetti, V. Delli Colli, and Y. Coia, "Design of axial flux PM synchronous machines through 3-D coupled electromagnetic thermal and fluid-dynamical finite-element analysis," *IEEE Trans. Ind. Electron.*, vol. 55, no. 10, pp. 3591–3601, Oct. 2008.
- [8] C. Buccella, C. Cecati, and F. de Monte, "A coupled electrothermal model for planar transformer temperature distribution computation," *IEEE Trans. Ind. Electron.*, vol. 55, no. 10, pp. 3583–3590, Oct. 2008.
- [9] Z. Makni, M. Besbes, and C. Marchand, "Multiphysics design methodology of permanent-magnet synchronous motors," *IEEE Trans. Veh. Technol.*, vol. 56, no. 4, pp. 1524–1530, Jul. 2007.
- [10] L. Encica, J. J. H. Paulides, E. A. Lomonova, and A. J. A. Vandenput, "Electromagnetic and thermal design of a linear actuator using output polynomial mapping," in *Conf. Rec. 41st IEEE IAS Annu. Meeting*, Oct. 8–12, 2006, vol. 4, pp. 1919–1926.
- [11] I.-C. Vese, F. Marignetti, and M. M. Radulescu, "Multiphysics approach to numerical modeling and analysis of permanent-magnet tubular linear motors," in *Proc. 18th ICEM*, Vilamoura, Portugal, Sep. 4–6, 2008, pp. 1–4.
- [12] "Electromagnetic field analysis software," JMag Studio 9.0—User's Manual Solver.
- [13] Y. Amara, J. Wang, and D. Howe, "Stator iron loss of tubular permanent-magnet machines," in *Conf. Rec. 39th IEEE IAS Annu. Meeting*, Oct. 2004, vol. 3, pp. 2119–2124.
- [14] I.-C. Vese, F. Marignetti, R. Di Stefano, and M. M. Radulescu, "Electromagnetic and thermal analysis of a small permanent-magnet tubular machine," in *Proc. 6th Int. Symp. LDIA*, Lille, France, Sep. 16–19, 2007, [CD-ROM].
- [15] B. Alvarenga, "Thermal characterization of long electrical devices—Application to a tubular linear induction motor," in *Proc. IEMDC*, Jun. 2003, vol. 2, pp. 938–942.
- [16] D. Staton, A. Boglietti, and A. Cavagnino, "Solving the more difficult aspects of electric motor thermal analysis in small and medium size industrial induction motors," *IEEE Trans. Energy Convers.*, vol. 20, no. 3, pp. 620–628, Sep. 2005.
- [17] K. J. Meessen, B. Gysen, J. Paulides, and E. A. Lomonova, "Halbach permanent magnet shape selection for slotless tubular actuators," *IEEE Trans. Magn.*, vol. 44, no. 11, pp. 4305–4308, Nov. 2008.
- [18] Z. Q. Zhu, X. Chen, D. Howe, and S. Iwasaki, "Electromagnetic modeling of a novel linear oscillating actuator," *IEEE Trans. Magn.*, vol. 44, no. 11, pp. 3855–3858, Nov. 2008.
- [19] B. Gysen, K. J. Meessen, J. Paulides, and E. A. Lomonova, "Semi-analytical calculation of the armature reaction in slotted tubular permanent magnet actuators," *IEEE Trans. Magn.*, vol. 44, pt. 1, no. 11, pp. 3213–3216, Nov. 2008.
- [20] Z. Gmyrek, A. Boglietti, and A. Cavagnino, "Iron loss prediction with PWM supply using low- and high-frequency measurements: Analysis and results comparison," *IEEE Trans. Ind. Electron.*, vol. 55, no. 4, pp. 1722–1728, Apr. 2008.
- [21] D. A. Staton and A. Cavagnino, "Convection heat transfer and flow calculations suitable for electric machines thermal models," *IEEE Trans. Ind. Electron.*, vol. 55, no. 10, pp. 3509–3516, Oct. 2008.
- [22] D. G. Dorrell, "Combined thermal and electromagnetic analysis of permanent-magnet and induction machines to aid calculation," *IEEE Trans. Ind. Electron.*, vol. 55, no. 10, pp. 3566–3574, Oct. 2008.



Ioana-Cornelia Vese received the Dipl.Ing. degree in electrical engineering from the Technical University of Cluj-Napoca, Cluj-Napoca, Romania, in 2003, where she is currently working toward the Ph.D. degree in the Special Electric Machines and Light Electric Traction Group.

Since 2007, she has been an Assistant Lecturer in the Department of Electric Drives and Robots, Technical University of Cluj-Napoca. Her research interests include multiphysics analysis by finite elements, linear tubular electric actuators, and design

and control strategies of electric motors.



Fabrizio Marignetti (M'00–SM'08) was born in Naples, Italy, on May 18, 1968. He received the Laurea (with honors) and Ph.D. degrees in electrical engineering from the University "Federico II," Naples, in 1993 and 1998, respectively.

In 1998, he joined the University of Cassino, Cassino, Italy, where he is currently an Associate Professor of power electronic converters, electrical machines, and drives and where he has been lecturing on electrical machine dynamics, electromechanical system design, and design of electric drives

for electric vehicles since 1996. He was bestowed a scholarship of rational mechanics by the University of Cassino. He has been a Scientific Coordinator of research contracts with public associations and industrial enterprises in the field of electrical machines and drives. He is a Member of the Editorial Board of the *Journal of Electrical Engineering* and is a Reviewer for many journals, including the *International Journal of Power and Energy Systems*. His scientific production is witnessed by 104 papers included both in international journals and in the proceedings of national and international conferences and by three patents. His research interests include design, analysis, and digital control of electrical machines.

Prof. Marignetti is a Reviewer for many journals, including the IEEE TRANSACTIONS ON INDUSTRY APPLICATIONS. He has been a member of the IEEE Industrial Electronics Society since December 1999.



Mircea M. Radulescu (M'94–SM'99) received the Dipl.Ing. degree in electrical engineering (with honors) from the Technical University of Cluj-Napoca, Cluj-Napoca, Romania, in 1978, and the Ph.D. degree in electrical engineering from the Polytechnic University of Timisoara, Timisoara, Romania, in 1993.

He was an Invited Professor at Helsinki University of Technology, Espoo, Finland, in 1997; at Rheinisch-Westfälische Technische Hochschule Aachen, Aachen, Germany, in 1999; at The University of Akron, Akron, OH, in 1999 and 2001; at the Université "Pierre et Marie Curie," Paris, France, in 2002; at the Université de Picardie "Jules Verne," Amiens, France, in 2003; and at the Ecole Centrale de Lille, Villeneuve d'Ascq, France, in 2006–2008. Since 1983, he has been with the Faculty of Electrical Engineering, Technical University of Cluj-Napoca, where he is currently a Full Professor in the Department of Electric Machines and the Head of the Special Electric Machines and Light Electric Traction Group. He is the author or coauthor of more than 120 published scientific papers in refereed technical journals and international conference and symposium proceedings. He is an Associate Editor of the international scientific quarterly *Electromotion*. His biography is listed in several editions of *Who's Who in the World* and *Who's Who in Science and Engineering*. His teaching and research activities include computer-aided design of electromechanical devices, field analysis of electromagnetic structures, the design and control of small electric motors, actuators and mechatronic drives, and light electric traction systems.

Prof. Radulescu is a member of the International Steering Committees of several conferences and symposia in the field of electric motor drives and electric traction.